PETROGRAPHY AND GEOCHEMISTRY OF NORTHWEST AFRICA (NWA) 15497, A NEWLY CLASSIFIED BASALTIC SHERGOTTITE. V. Mugica[1] and D. Sheikh[2], (vthomas50@csu.fullerton.edu), [1]California State University, Fullerton, Department of Geological Science, CA, 92831, USA. [2]Cascadia Meteorite Laboratory, Portland State University, Department of Geology, Portland, OR 97239, USA.

Introduction: Martian meteorites are currently the only samples we have from Mars that allow us to better understand the nature of magmatic mobilization in Martian igneous plumbing systems throughout the Martian interior [1]. Existing collections of Martian meteorites currently number 346 known specimens as recorded in the Meteoritical Bulletin Database (lpi.usra.edu) with 11 distinct ejection events documented [1]. Shergottites represent the most abundant group of Martian meteorites and are texturally classified into four primary sub-types (poikilitic, basaltic, gabbroic and olivine-phyric) on the basis of texture (grain size, habit and modal proportions), and geochemically grouped based on their relative depletion or enrichment in incompatible trace elements (ITE) and isotopic abundances [1]. Shergottites are comprised of phases in different proportions such as maskelynite (shocked plagioclase), augite, pigeonite, orthopyroxene, olivine and accessory phases such as Cr-spinel, phosphates (merrillite, apatite), sulfides, titanomagnetite, ilmenite, baddeleyite and silica. Here we provide a detailed analysis of Northwest Africa (NWA) 15497, a newly classified basaltic shergottite (Fig. 1), with potential implications on its petrogenesis.

Fig. 1. *Hand specimen image of NWA 15497 with unweathered, shiny fusion crust.*

Petrography: NWA 15497 has a subophitic texture comprised of subhedral, complexly zoned pyroxene (avg. grain size = 0.38 mm; n=79) and maskelynite (avg. grain size = 0.71 mm; n=54) set within a fine-grained matrix that includes abundant accessory chlorapatite, merrillite, titanomagnetite, troilite, silica glass and mesostasis. Pyroxene grains throughout the sample show prismatic and equant habits (Figs. 2-3).

NWA 15497 contains a compositionally mixed shock melt pocket (1.70 mm in longest axis) found in other Martian shergottites [2] (Fig. 4). Maskelynite in the sample displays equant and prismatic habits.

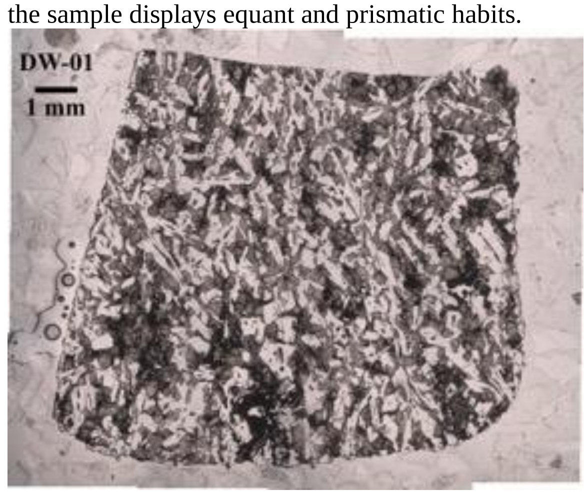

Fig. 2. *Plane polarized light image of NWA 15497.*

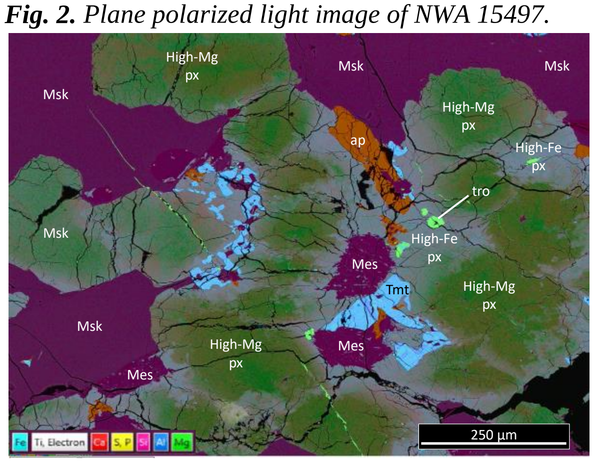

Fig. 3. *False color EDS chemical map of the different phases in NWA 15497. Phases are abbreviated as Mes=mesostasis, ap=chlorapatite, px=pyroxene, tro=troilite, Tmt=titanomagnetite, Msk=maskelynite.* Element color key and scale bar displayed.

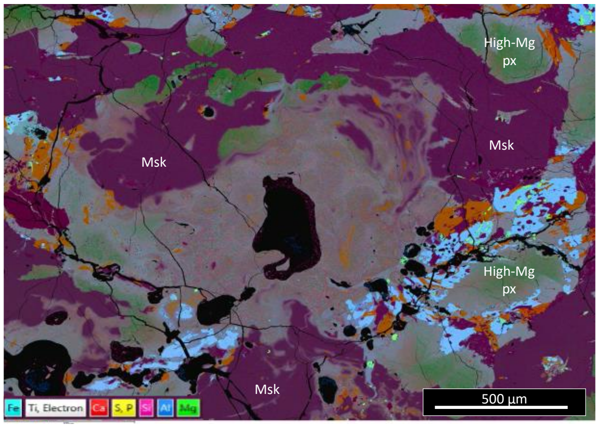

Fig. 4. *Figure shows a false color EDS chemical map of a compositionally mixed (albeit gray colored) Fe-rich shock melt pocket. Abbreviations are Msk=maskelynite, px=pyroxene.* Color key same as Fig 3.

Mineral Chemistry: The complex zonation of the pyroxene is characterized by high-Mg cores trending to Fe-rich rims consistent with other basaltic shergottites documented such as NWA 8657, NWA 2975 and NWA 5298 [6-8] (Fig. 3). Pyroxene also show irregular compositional zones containing Ca-rich and Ca-poor areas similar to Los Angeles [3]. Average pigeonite compositions in NWA 15497 are $Fs_{59.0\pm15.1}Wo_{17.4\pm3.4}$ with ranges of $Fs_{32.2-83.9}Wo_{10.9-24.9}$ and Fe/Mn=35±4 (n=95), Average high-Ca pyroxene compositions are $Fs_{35.8\pm9.6}Wo_{29.7\pm3.0}$ with ranges of $Fs_{25.9-60.5}Wo_{25.0-35.0}$ and Fe/Mn=31±4 (n=29). Pyroxene Fe/Mn ratios are indicative of Martian planetary provenance [4,5]. NWA 15497 pyroxene compositions have more widely distributed minima and maxima compared to pyroxene found in other basaltic shergottites such as NWA 5298 ($En_{58-3}Wo_{36-10}$), NWA 2975 (pigeonite ranges from $Fs_{43-63}Wo_{12-17}$ and augitic ranges of $Fs_{23-49}Wo_{27-36}$) and NWA 8657 (with core-to-rim compositions of $En_{60-20}Fs_{22-60}$) [6-8].

Maskelynite in NWA 15497 displays compositions of $An_{48.2\pm4.5}Or_{2.7\pm1.6}$ with ranges between $An_{40.8-54.1}Or_{1.3-8.4}$ (n=33). The An contents of maskelynite found in NWA 15497 has a larger compositional range compared to An values of maskelynite reported in NWA 8657 (~An_{56-58} and ~An_{52-54}) and NWA 2975 (~$An_{52-55}Or_1$) but similar to NWA 5298 (An_{40-55}) and Los Angeles ($An_{56–38}Ab_{43–56}Or_{1–7}$) [6-9].

Discussion: Based on the abundances of pyroxene and maskelynite (and the presence of accessory phases such as chlorapatite, merrillite, titanomagnetite, troilite, silica glass, mesostasis) and the similar compositions of these phases to those in other documented basaltic shergottites [6-9], we conclude that NWA 15497 is a basaltic shergottite. The complex zonation of the pyroxene is characterized by high-Mg cores trending to Fe-rich rims consistent with other basaltic shergottites documented such as NWA 8657, NWA 2975 and NWA 5298 [6-8] (Fig. 3). Pyroxene grains also show irregular compositional zones containing Ca-rich and Ca-poor areas as well as resorption textures along the margins of the Mg-rich cores indicating disequilibrium processes during crystallization. NWA 5298 has been suggested by [8] to have crystallized from a continuously fractionating melt in a closed magmatic system, whereas [6] invoke pyroxene grains becoming resorbed during entrainment and emplacement to the surface; based on our preliminary work, either model is feasible for the petrogenesis and pyroxene disequilibrium textures observed in NWA 15497. Based on maskelynite compositions, the protolith plagioclase likely underwent shock metamorphism of ~29 GPa during the impact ejection event of NWA 15497 [10].

Acknowledgments: This work would not have been possible if it wasn't for the generosity and guidance provided by Daniel Sheikh.

References: [1] Udry et al. (2020) *JGR Planets*, 125. [2] Walton et al. (2009) *MAPS*, *44*, 55-76. [3] Mikouchi et al. (2001) *Antarct. Meteorite Res.*, *14*, 1-20. [4] Papike et al. (2003) *LPSC XXXIV*, abstract #1018. [5] Papike et al. (2009) *GCA*, *73*, 7443-7485. [6] Howarth et al. (2018) *MAPS*, *53*, 249-267. [7] He et al. (2015) *MAPS*, *50*, 2024-2044. [8] Hui et al. (2011) *MAPS*, *46*, 1313-1328. [9] Rubin et al. (2000) *Geology*, *v. 28*, 1011-1014. [10] Fritz et al. (2019) *MAPS*, *54*, 1533-1547.